Rotational level structure of sodium isotopes inside the "island of inversion"

P. Doornenbal[1,*], H. Scheit[1,2], S. Takeuchi[1], Y. Utsuno[3], N. Aoi[1], K. Li[1,2], M. Matsushita[1], D. Steppenbeck[1], H. Wang[1,2], H. Baba[1], E. Ideguchi[4], N. Kobayashi[5], Y. Kondo[5], J. Lee[1], S. Michimasa[4], T. Motobayashi[1], T. Otsuka[4,5], H. Sakurai[1], M. Takechi[1], Y. Togano[1], and K. Yoneda[1]

[1]*RIKEN Nishina Center, Wako, Saitama 351-0198, Japan*
[2]*Peking University, Beijing 100871, P.R. China*
[3]*Advanced Science Research Center, Japan Atomic Energy Agency, Tokai, Ibaraki 319-1195, Japan*
[4]*Center for Nuclear Study, University of Tokyo, RIKEN Campus, Wako, Saitama 351-0198, Japan*
[5]*Department of Physics, Tokyo Institute of Technology, Meguro, Tokyo 152-8551, Japan*
*E-mail: pieter@ribf.riken.jp

. . . .
The neutron-rich nuclei ^{33,34,35}Na were studied via in-beam γ-ray spectroscopy following nucleon removal reactions from a ^{36}Mg secondary beam at $\sim$220 MeV/u. Excited states of ^{34,35}Na are reported for the first time. A third transition was observed for ^{33}Na in addition to the known $7/2_1^+ \to 5/2_1^+ \to 3/2_{g.s.}^+$ cascade and is suggested to be the $9/2_1^+ \to 7/2_1^+$ transition. Similarly, a $7/2_1^+ \to 5/2_1^+ \to 3/2_{g.s.}^+$ cascade is proposed for the decay pattern observed for ^{35}Na. The transition energy ratios are close to expectation values for $K = 3/2$ rotational bands in the strong coupling limit. Comparisons to large-scale shell model calculations in the sd–pf model space support the spin–parity assignments.
. . . .

Subject Index   D13, D27

1. Introduction

The study of neutron-rich Ne, Na, and Mg nuclei around the breakdown of the $N = 20$ neutron magic number, an area in the Segré chart termed the "island of inversion" [1], has provided a wealth of information on the evolution of nuclear shell structure away from the valley of β stability. A consequence of the reduced $N = 20$ neutron shell gap is a gain in energy by $\nu(sd)^{-2}pf^2$ "intruder" configurations in the ground state. They represent the main feature for nuclei belonging to the "island of inversion" [2], while the $N = 20$ shell quenching itself can be attributed to spin–isospin components of the nucleon–nucleon interaction [3]. More specifically, an attractive monopole interaction between the $\pi 0d_{5/2}$ and $\nu 0d_{3/2}$ orbitals originating from the tensor force results in a reduced $N = 20$ gap when protons are removed from the $0d_{5/2}$ orbital [4].

Due to its location in the proximity of the neutron drip-line, accessing the "island of inversion" is an experimental challenge. Therefore, although many experiments have investigated the onset of collectivity for nuclei located at the "Western" borderline at $N = 19, 20$, only a few experiments have been directed at the originally proposed "Eastern" boundary at $N = 22$ [1,2] via inelastic scattering and knockout reactions [5–11]. Beyond $N = 22$, excited states have been reported only for Mg isotopes [12,13] and indicate a continuous deformation inferred from low 2_1^+ energies and large

energy ratios for the 4_1^+ and 2_1^+ levels. Shell model calculations predict that nuclei with $N > 22$ and lower element numbers are also deformed [14–16]. However, no experimental data exist for these nuclei.

Several in-beam γ-ray experiments have been performed in the past, targeting neutron-rich sodium isotopes in the vicinity of the "island of inversion" [7–9,17,18]. For odd-A isotopes, low-lying $3/2^+$ and $5/2^+$ configurations compete for the ground state, the latter succeeding only for ^{27,29}Na (see, e.g., Fig. 6 of Ref. [7]). Ground-state spins were firmly assigned up to ^{31}Na [19]. The heaviest sodium isotope with a measured spin for at least one of its excited states is ^{30}Na. Here, 1^+ levels could be identified from high logft values in the β decay of ^{30}Ne [20,21]. On the other hand, spin assignments for sodium isotopes within the "island of inversion" are based on the aid from the shell model and are thus only tentative. To assure the validity of the utilized interactions, the availability of larger experimental data sets is of interest. In this paper, we report on the first γ-ray spectroscopy performed for the $N = 23, 24$ sodium isotopes ^{34,35}Na and a new transition in ^{33}Na. For the latter nucleus, previous measurements suggested that the observed two transitions originate from a $7/2_1^+ \rightarrow 5/2_1^+ \rightarrow 3/2_{g.s.}^+$ cascade and the energy ratio was found to be close to an ideal $K = 3/2$ rotational band in the strong coupling limit [9].

2.   Experiment

The experiment was performed at the Radioactive Isotope Beam Factory, operated by the RIKEN Nishina Center and the Center for Nuclear Study, University of Tokyo. A ^{48}Ca beam with an average intensity of 70 particle nA was accelerated by the superconducting ring cyclotron (SRC) to 345 MeV/u and incident on a 15 mm thick beryllium production target. A combination of two magnetic dipoles and a 15 mm thick aluminum degrader was utilized to filter a ^{36}Mg secondary beam with the BigRIPS fragment separator [22] by applying the $B\rho–\Delta E–B\rho$ method. Particle identification of the secondary beams was performed with the second stage of BigRIPS, as described in previous experiments [23,24]. For further purification, a second aluminum degrader of 5 mm thickness was inserted at the dispersive focal point of the second BigRIPS stage. After passing BigRIPS, the secondary beams were incident on 2.54 g/cm^2 carbon and 2.13 g/cm^2 CH$_2$ (polyethylene) reaction targets, respectively. BigRIPS was operated with its full momentum acceptance of $\pm 3\%$ and the average intensity of ^{36}Mg was 90 particles per second.

Gamma-rays emitted in coincidence with the secondary reactions were detected with the DALI2 array [25], which was composed of 186 large-volume NaI(Tl) detectors. To maximize the γ-ray detection efficiency, DALI2 covered a large fraction of the solid angle with center-of-crystal angles ranging from 19 to 149 degrees relative to the beam axis. As the average energy of the ^{36}Mg fragments was 236 MeV/u in front of the reaction target and also inelastic scattering channels were of interest, it was necessary to suppress bremsstrahlung background by covering the beam tube with 1 mm of Pb and setting the energy thresholds for the DALI2 detectors to about 200 keV. Calibration and efficiency measurements for DALI2 were performed using ^{60}Co, ^{88}Y, and ^{137}Cs stationary sources, yielding an intrinsic resolution of 7% (FWHM) at 1 MeV. The obtained efficiency values were reproduced with simulations using the GEANT4 framework [26] with a maximum relative deviation of 5%. For a 1 MeV γ-ray emitted in-flight at $v/c = 0.58$, an energy resolution and full energy peak efficiency of 10% (FWHM) and 20%, respectively, were anticipated from GEANT4 simulations for events with γ-ray interactions in a single crystal only.
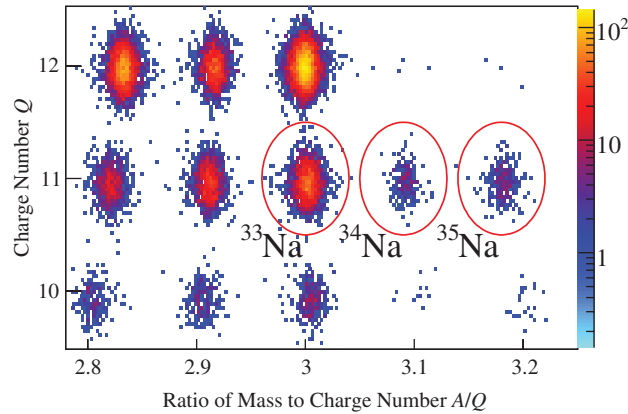
Fig. 1. Particle identification plot behind the secondary target using the ZeroDegree beam line detectors. A gate was applied on the ^{36}Mg secondary beam identified with BigRIPS and a coincident γ-ray was required in DALI2. The ^{33,34,35}Na reactions residues are indicated.

A second particle identification was required for the secondary reaction products and was performed with the magnetic spectrometer ZeroDegree with the $B\rho$–ΔE–TOF method [22]. Figure 1 shows clear separation in charge Q and mass-to-charge ratio A/Q for the three sodium isotopes of interest from other reaction products for the carbon target run. At least one coincident γ-ray was required to be detected in DALI2. The magnetic rigidity of ZeroDegree was set for ^{36}Mg. Reaction products of ^{34,35}Na, whose magnetic rigidity deviated significantly for the center of their respective momentum distribution, were thus largely cut by the ZeroDegree acceptance of $\pm 4\%$. Hence, the production cross-sections for these nuclei could not be determined. For ^{33}Na, which has the same $A/Q = 3$ as the ^{36}Mg secondary beam, production cross-section determinations were impeded by a plastic scintillator installed in front of the ΔE detector.

Gamma-ray energy spectra after Doppler correction and in coincidence with the ^{33,34,35}Na fragments detected in ZeroDegree are displayed in Fig. 2. Beta-values for the Doppler correction were calculated to the center of the reaction target from the measured velocities in ZeroDegree for the respective reaction residues. Due to the different momentum selection, the average β values varied by $\sim 2\%$ for the ^{33,34,35}Na fragments transmitted through ZeroDegree. In Fig. 2, all spectra were fitted with simulated response curves using the GEANT4 framework on top of two exponential background curves. Two γ-ray decays have been reported in earlier works at 429(5) and 688(6) keV in ^{33}Na [7,9], which were observed in the present work at 425(5) and 690(13) keV, respectively. These transitions were assigned in Ref. [9] to the $5/2_1^+ \rightarrow 3/2_{g.s.}^+$ and $7/2_1^+ \rightarrow 5/2_1^+$ decays based on the level systematics of the odd–even Na isotopes and comparison to shell model calculations using the SDPF-M effective interaction and the Monte Carlo Shell Model (MCSM) approach [16]. In the present work, a third γ-ray transition was observed for ^{33}Na in addition at 760(13) keV, which forms a doublet with the $7/2_1^+ \rightarrow 5/2_1^+$ decay. Gates on the γ-ray multiplicity M_γ, shown in the insets of Fig. 2, reveal that the new transition is predominantly observed for $M_\gamma = 3$ events. This feature, the MCSM predictions of Ref. [9], and the shell model calculations discussed below support a $9/2_1^+ \rightarrow 7/2_1^+$ assignment. For the odd–odd nucleus ^{34}Na, a single γ-ray transition was observed at 451(7) keV, while the energy spectrum of ^{35}Na exhibits excited states at 373(5) and 641(16) keV. The latter two transitions are suggested to form a $7/2_1^+ \rightarrow 5/2_1^+ \rightarrow 3/2_{g.s.}^+$ cascade as for ^{33}Na based on the shell model calculations presented below.
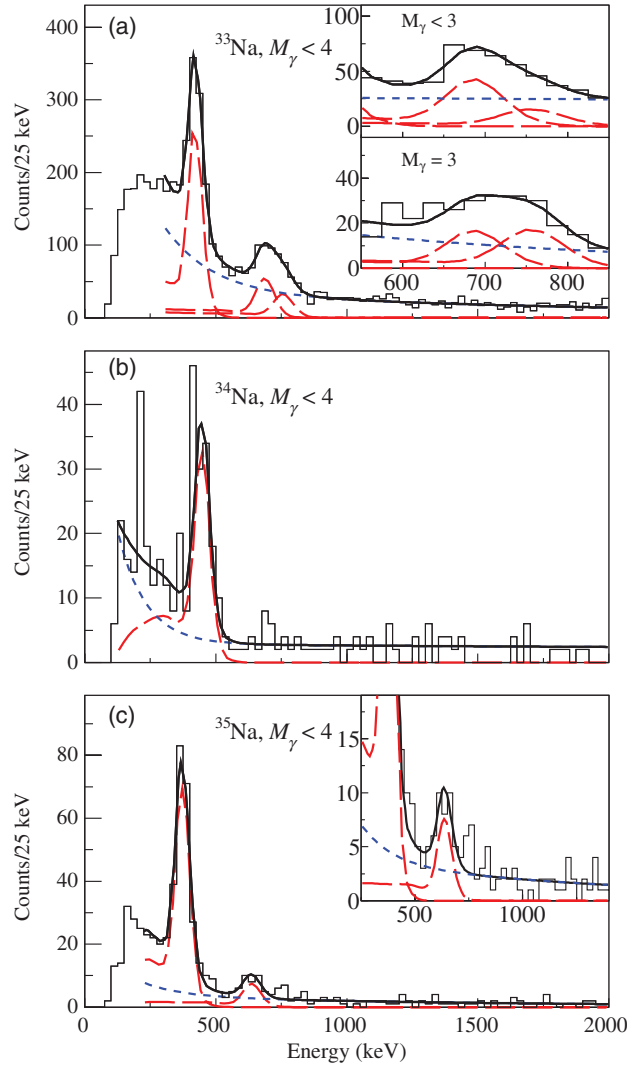
Fig. 2. Doppler-shift-corrected γ-ray energy spectra in coincidence with ^{33}Na (a), ^{34}Na (b), and ^{35}Na (c) detected in the ZeroDegree spectrometer following reactions in the carbon and polyethylene targets. Events with a maximum γ-ray multiplicity of $M_\gamma < 4$ were analyzed. The insets show for ^{33}Na that the transition at 760(13) keV is predominantly observed for $M_\gamma = 3$ events. All spectra were fitted (black solid lines) with simulated detector response curves (red long dashed lines) on top of two exponentials for the background (blue short dashed lines).

Transition energy errors in this work originate from energy calibration uncertainties ($\sim$3 keV), the unknown lifetime of the excited states ($\sim$1%), and the statistical errors of the peak fits.

3. Discussion

Energy level systematics of the odd–even sodium isotopes ^{31,33,35}Na including the proposed placements of the newly observed levels from this work are displayed in Fig. 3. They show remarkably little variation as a function of the neutron number. The excitation energy pattern as a function of the neutron number presented here resembles the constant level structure recently identified for the chain of magnesium isotopes up to $N = 26$ [12]. For these nuclei, $E(4_1^+)/E(2_1^+)$ ratios $R_{4/2} \approx 3$ were observed, indicative of a large deformation. In the case of the odd-A sodium nuclei, energy difference ratios of $[E(7/2_1^+) - E(3/2_{g.s.}^+)]/[E(5/2_1^+) - E(3/2_{g.s.}^+)] = 2.4$ and $[E(9/2_1^+) -$
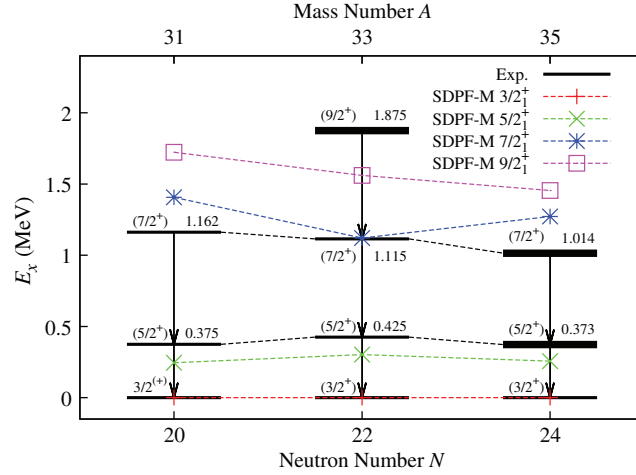
Fig. 3. Energy level systematics of the odd–even sodium isotopes ^{31,33,35}Na in comparison to shell model calculations using the SDPF-M effective interaction. Data are from this work (shown in bold) and Refs. [7,9,17]. Lines are drawn to guide the eye.

Table 1. Calculated energies levels (in MeV) with the SDPF-M effective interaction for ^{31,33,35}Na and neutron occupation numbers for the $0f_{7/2}$ and $1p_{3/2}$ orbitals. Only yrast and positive parity states are listed.

	^{31}Na			^{33}Na			^{35}Na		
J^π	E_x	$0f_{7/2}$	$1p_{3/2}$	E_x	$0f_{7/2}$	$1p_{3/2}$	E_x	$0f_{7/2}$	$1p_{3/2}$
$3/2^+_{g.s.}$	0	1.83	0.57	0	2.96	1.06	0	3.70	1.80
$5/2^+_1$	0.245	1.84	0.51	0.303	2.98	1.01	0.256	3.72	1.75
$7/2^+_1$	1.407	1.75	0.65	1.121	3.00	1.05	1.272	3.67	1.82
$9/2^+_1$	1.724	1.79	0.53	1.561	3.03	1.01	1.455	3.72	1.80
$1/2^+_1$	2.305	1.86	0.48	2.440	2.79	1.31	1.441	3.68	2.21

$E(3/2^+_{g.s.})]/[E(7/2^+_1) - E(3/2^+_{g.s.})] = 1.75$ are expected for $K = 3/2$ rotational bands in the strong coupling limit. Experimentally, ratios of 3.10(4), 2.62(4), and 2.72(6) are obtained for the former in ^{31,33,35}Na, and 1.68(3) for the latter in ^{33}Na, consistent with an assumption of $K = 3/2$ rotational bands, at least for ^{33,35}Na.

Only the ground state spin of ^{31}Na has been determined [19]. In addition, an intermediate-energy Coulomb excitation experiment concluded that a first excited state spin of $5/2^+$ was most probable [17]. Other spin assignments were made based on shell model comparisons [7,9]. Following this approach, we present here shell model calculations for ^{31,33,35}Na using the SDPF-M effective interaction [16,27], comprising a model space of $0d_{5/2}$, $1s_{1/2}$, and $0d_{3/2}$ orbitals for protons and neutrons as well as $0f_{7/2}$ and $1p_{3/2}$ orbitals for neutrons. In contrast to earlier works that calculated level energies in the sodium isotopes using SDPF-M with the MCSM [9,27,28], however, exact diagonalization of the Hamiltonian matrix was performed. The calculated energy levels are presented in Table 1 and shown in Fig. 3 together with experimental level schemes. The $5/2^+_1$ levels are found to be about 100 keV lower than those given by the experimental results. It is interesting to note that, for ^{33}Na, the MCSM predicted the $5/2^+_1$ level at 390 keV [9], closer to the experimental value of 429 keV than the exact diagonalization. For the $7/2^+_1$ levels, the deviation from experiment shifts in the opposite

Table 2. Calculated B(E2) and B(M1) strengths (in $e^2 fm^4$ and μ_N^2) for ^{31,33,35}Na using the SDPF-M effective interaction.

$J_i^\pi \rightarrow J_f^\pi$	^{31}Na		^{33}Na		^{35}Na	
	B(E2)	B(M1)	B(E2)	B(M1)	B(E2)	B(M1)
$3/2_{g.s.}^+ \rightarrow 5/2_1^+$	199.7	0.373	253.3	0.570	239.6	0.380
$3/2_{g.s.}^+ \rightarrow 7/2_1^+$	97.5		128.7		130.5	
$5/2_1^+ \rightarrow 7/2_1^+$	82.3	0.489	122.8	0.636	65.9	0.390
$5/2_1^+ \rightarrow 9/2_1^+$	119.8		158.4		158.0	
$7/2_1^+ \rightarrow 9/2_1^+$	53.3	0.909	86.4	1.060	81.9	0.608
$1/2_1^+ \rightarrow 3/2_{g.s.}^+$	8.8	0.003	11.7	0.002	14.9	0.002
$1/2_1^+ \rightarrow 5/2_1^+$	20.4		13.8		30.7	

direction with over-prediction up to $\sim$250 keV for ^{31,35}Na. Finally, for the proposed $9/2_1^+$ level in ^{33}Na, the excitation energy is again under-predicted by $\sim$250 keV. Overall, the predictions from the SDPF-M interaction are in good agreement with the excited levels in ^{31,33,35}Na, yielding a mean level deviation of $\sim$170 keV.

Reduced transition probabilities B(E2) and B(M1) were calculated to corroborate decay patterns and spin assignments as well as to study the expected collectivity in the sodium isotopes. Effective charges for protons and neutrons of $e_p = 1.3e$ and $e_n = 0.5e$ were utilized. The results are shown in Table 2 and confirm the suggested cascades due to the dominance of $\Delta I = 1$ transitions and large B(M1) values. Using the experimental transition energies and calculated B(E2) and B(M1) values results in estimated $7/2_1^+ \rightarrow 3/2_{g.s.}^+$ branching ratios of 4, 5, and 6% relative to the $7/2_1^+ \rightarrow 5/2_1^+$ decay. These ratios are too small to be sensitive to the present setup for ^{33,35}Na. Similarly, the $9/2_1^+ \rightarrow 5/2_1^+$ branching in ^{33}Na is calculated to be 10% relative to the $9/2_1^+ \rightarrow 7/2_1^+$ transitions. Regarding the calculated transition probabilities, we further note that, using the equations presented in Ref. [17] for a rotational model, the calculated B(E2) values in ^{31}Na for $3/2_{g.s.}^+ \rightarrow 5/2_1^+$ and $5/2_1^+ \rightarrow 7/2_1^+$ correspond to deformations of $\beta = 0.51$ and $\beta = 0.46$, respectively, in agreement with the experimental findings of $\beta = 0.59(10)$ in the intermediate energy Coulomb excitation experiment. Similar B(E2) values have been calculated for ^{33,35}Na, suggesting that these nuclei are comparable in deformation.

A spin assignment to spin $7/2^+$ for the second excited state in ^{35}Na needs particular justification, as its direct population is not expected from sd-shell proton knockout reactions. The neutron separation energy is only $S_n = 1520(300)$ keV [29], which leaves little space for feeding transitions. The SDPF-M interaction predicts the $1/2_1^+$ state at 1.441 MeV with comparable B(E2) to the $3/2_{g.s.}^+$ and $5/2_1^+$ states. Given the much larger transition energy of the former, a direct ground state decay is expected to be dominant. In the experimental spectrum, however, no indication for a γ-ray transition at $\sim$1 MeV was observed. On the other hand, a recent study of the $1p$-knockout reaction from ^{16}C revealed the population of the $5/2_1^-$ and $7/2_1^-$ states in ^{15}B with 10% of the inclusive cross-section [30]. This is not anticipated from the removal of protons from $spsd$ shell model orbitals and the momentum distribution of these excited states was found to be lower than for the ground state [30]. In low-beam-energy projectile fragmentation, the appearance of low energetic tails of the momentum distribution was attributed to inelastic, non-direct processes [31–34]. More generally, projectile fragmentation is regarded as a three-step process involving friction due to kinetic
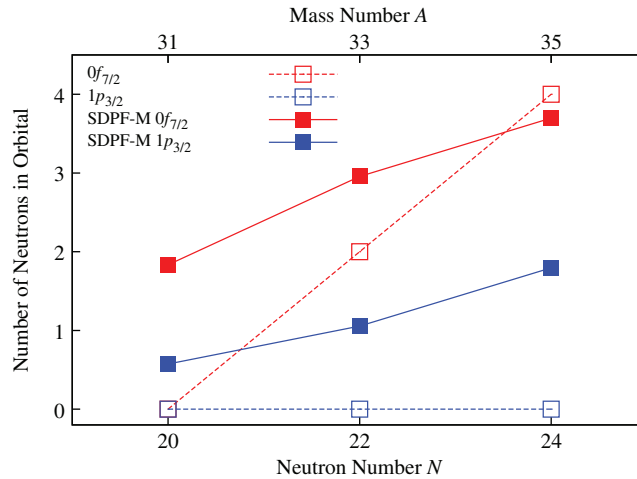
Fig. 4. Calculated ground state occupation numbers for neutron $0f_{7/2}$ (filled red squares) and $1p_{3/2}$ (filled blue squares) orbitals using the SDPF-M interaction. Normal filling is indicated by the open red and blue squares for the $0f_{7/2}$ and $1p_{3/2}$ orbitals, respectively.

energy loss, exchange of nucleons, and transformation into internal degrees of freedom [35]. Similarly, for deeply bound nucleon removal reactions, "forbidden" states may arise from these dissipative processes during the core-target collision time. Note that in this case the reaction occurs at the projectile surface with significant spatial overlap with the target, which may increase the probability of nucleon rearrangement, in contrast to loosely bound nucleon removal reactions. In the present work, the momentum selection for ZeroDegree was set 6% lower than the maximum for ^{35}Na and thus accepted mainly the low momentum tail. As observed for ^{15}B, the population of a "forbidden" $7/2^+$ state may be enhanced in this region of the momentum distribution.

An important aspect of describing nuclei in the vicinity of the "island of inversion" is the number of neutrons promoted from the sd to the pf shell that drives the deformation in these nuclei. The occupation numbers of neutrons in the $0f_{7/2}$ and $1p_{3/2}$ orbitals, given in Table 1 for the ground and excited states, reveal that this number gradually decreases from ~ 2.4 in ^{31}Na to ~ 1.5 in ^{35}Na in comparison to a "normal" filling. Furthermore, as shown in Fig. 4, the increased level occupancy shifts from an excess of the $0f_{7/2}$ orbital at $N = 20$ to the $1p_{3/2}$ orbital at $N = 24$. This pattern corresponds again to the magnesium isotopes, where a shift from $0f_{7/2}$ to $1p_{3/2}$ excess was also calculated and interpreted as a merge of the $N = 20$, 28 shell quenchings [14].

In a one-neutron knockout study, a narrow longitudinal momentum distribution of ^{32}Mg residues revealed significant $1p_{3/2}$ neutron contributions [36]. The obtained data could not be reproduced with spectroscopic factors of the SDPF-M interaction calculated with the MCSM. To ameliorate the agreement, the $1p_{3/2}$ orbital was shifted down in energy by 0.8 MeV and $0f_{7/2}$ up in energy by 0.2 MeV, resulting in a relative narrowing by 1 MeV. With this modified SDPF-M interaction, excited $5/2_1^+$, $7/2_1^+$, and $9/2_1^+$ states are calculated to be at 0.296, 1.361, and 1.751 MeV for ^{31}Na, at 0.348, 1.201, and 1.667 MeV for ^{33}Na, and at 0.294, 1.249, and 1.526 MeV for ^{35}Na. A mean level deviation of ~ 140 keV is now obtained for the known excited states, corresponding to an improvement of 30 keV. Thus, the excitation energies observed in the neutron-rich sodium isotopes support the suggested shift in the $1p_{3/2}$ single particle energies, though part of the deviations may be explained from other sources.

Few conclusions can be drawn from the γ-ray transition observed in ^{34}Na. Shell model calculations with the unmodified SDPF-M interaction yield a $J^\pi = 2^-$ ground state. Yrast 4^-, 3^-, 1^-, 5^-, and 0^- negative parity states lie at 0.090, 0.106, 0.297, 0.527, and 0.583 MeV, respectively. Positive parity 0^+, 2^+, 1^+, 3^+, 4^+, and 5^+ yrast states are found at 0.289, 0.641, 0.777, 0.956, 1.392, and 2.110 MeV, respectively. Due to the high level density, it is impossible to conclude which γ-ray transition has been observed. A determination of the ground state spin and parity may help to put further constraints on the nature of the observed γ-ray transition in ^{34}Na.

4.   Conclusion

In summary, excited states in the neutron-rich sodium isotopes ^{33,34,35}Na were observed following nucleon removal reaction of a ^{36}Mg secondary beam at $\sim$220 MeV/u. For ^{33}Na, a new γ-ray transition was observed in addition to the known $5/2_1^+ \rightarrow 3/2_{g.s.}^+$ and $7/2_1^+ \rightarrow 5/2_1^+$ transitions and assigned to the $9/2_1^+ \rightarrow 7/2_1^+$ decay. Excited states in ^{34,35}Na were reported for the first time. For the odd–odd nucleus ^{34}Na, the interpretation of the observed transition at 451(7) keV remains ambiguous, while the level structure of odd–even sodium isotopes was found to be well described by the SDPF-M effective interaction. The proposed level structure of the most neutron-rich sodium isotope spectroscopically studied to date, ^{35}Na, is similar to the ones for ^{31,33}Na and can be interpreted as a rotational band in the $K = 3/2$ strong coupling limit. This implies large deformation to at least neutron number $N = 24$ for the sodium isotopes and suggests merging of the $N = 20$ and $N = 28$ shell quenching, as seen in the neutron-rich magnesium isotopes [12].

References

[1]   E. K. Warburton, J. A. Becker, and B. A. Brown, Phys. Rev. C, **41**, 1147 (1990).
[2]   A. Poves and J. Retamosa, Phys. Lett. B, **184**, 311 (1987).
[3]   T. Otsuka, R. Fujimoto, Y. Utsuno, B. Alex Brown, M. Honma, and T. Mizusaki, Phys. Rev. Lett., **87**, 082502 (2001).
[4]   T. Otsuka, T. Suzuki, R. Fujimoto, H. Grawe, and Y. Akaishi, Phys. Rev. Lett., **95**, 232502 (2005).
[5]   J. A. Church et al., Phys. Rev. C, **72**, 054320 (2005).
[6]   P. Doornenbal et al., Phys. Rev. Lett., **103**, 032501 (2009).
[7]   P. Doornenbal et al., Phys. Rev. C, **81**, 041305(R) (2010).
[8]   Z. Elekes et al., Phys. Rev. C, **73**, 044314 (2006).
[9]   A. Gade et al., Phys. Rev. C, **83**, 044305 (2011).
[10]   H. Iwasaki et al., Phys. Lett. B, **522**, 227 (2001).
[11]   K. Yoneda et al., Phys. Lett. B, **499**, 233 (2001).
[12]   P. Doornenbal et al., Phys. Rev. Lett., **111**, 212502 (2013).
[13]   A. Gade et al., Phys. Rev. Lett., **99**, 072502 (2007).
[14]   E. Caurier, F. Nowacki, and A. Poves, arXiv:1309.6955.
[15]   A. Poves, E. Caurier, F Nowacki, and K Sieja, Phys. Scripta T, **150**, 014030 (2012).
[16]   Y. Utsuno, T. Otsuka, T. Mizusaki, and M. Honma, Phys. Rev. C, **60**, 054315 (1999).
[17]   B. V. Pritychenko, T. Glasmacher, B. A. Brown, P. D. Cottle, R. W. Ibbotson, K. W. Kemper, L. A. Riley, and H. Scheit, Phys. Rev. C, **63**, 011305 (2000).
[18]   B. V. Pritychenko, T. Glasmacher, P. D. Cottle, R. W. Ibbotson, K. W. Kemper, K. L. Miller, L. A. Riley, and H. Scheit, Phys. Rev. C, **66**, 024325 (2002).

[19] M. Keim, U. Georg, A. Klein, R. Neugart, M. Neuroth, S. Wilbert, P. Lievens, L. Vermeeren, and B. A. Brown, Eur. Phys. J. A, **8**, 31 (2000).
[20] A. T. Reed et al., Phys. Rev. C, **60**, 024311 (1999).
[21] V. Tripathi et al., Phys. Rev. C, **76**, 021301(R) (2007).
[22] T. Kubo et al., Prog. Theor. Exp. Phys., **2012**, 03C003 (2012).
[23] N. K. Kobayashi et al., Phys. Rev. C, **86**, 054604 (2012).
[24] T. Ohnishi et al., J. Phys. Soc. Jpn., **77**, 083201 (2008).
[25] S. Takeuchi, T. Motobayashi, H. Murakami, K. Demichi, and H. Hasegawa, Development of NaI(Tl) detector array for in-beam γ-ray spectroscopy, In *RIKEN Accelerator Progress Report*, (RIKEN, Wako, Japan, 2003), Vol. 36, p. 148.
[26] S. Agostinelli et al., Nucl. Instrum. Meth. A, **506**, 250 (2003).
[27] Y. Utsuno, T. Otsuka, T. Glasmacher, T. Mizusaki, and M. Honma, Phys. Rev. C, **70**, 044307 (2004).
[28] Y. Utsuno, T. Otsuka, T. Mizusaki, and M. Honma, Nucl. Phys. A, **704**, 50c (2002).
[29] A. H. Wapstra, F. G. Kondev, M. MacCormick, X. Xu, M. Wang, G. Audi, and B. Pfeiffer, Chin. Phys. C, **36**, 1603 (2012).
[30] F. Flavigny, A. Obertelli, A. Bonaccorso, G. F. Grinyer, C. Louchart, L. Nalpas, and A. Signoracci, Phys. Rev. Lett., **108**, 252501 (2012).
[31] V. Borrel, D. Guerreau, J. Galin, B. Gatty, D. Jacquet, and X. Tarrago, Z. Phys. A, **314**, 191 (1983).
[32] Y. Blumenfeld, J. C. Roynette, Ph. Chomaz, N. Frascaria, J. P. Garron, and J. C. Jacmart, Nucl. Phys. A, **445**, 151 (1985).
[33] F. Rami, J. P. Coffin, G. Guillaume, B. Heusch, P. Wagner, A. Fahli, and P. Fintz, Nucl. Phys. A, **444**, 325 (1985).
[34] Y. Périer, B. Lott, J. Galin, E. Liénard, M. Morjean, N. A. Orr, A. Péghaire, B. M. Quednau, and A. C. C. Villari, Phys. Lett. B, **459**, 55 (1999).
[35] O. Tarasov, Nucl. Phys. A, **734**, 536 (2004).
[36] R. Kanungo et al., Phys. Lett. B, **685**, 253 (2010).